Jehad Ahmad Yamin
yamin@ju.edu.jo
University of Jordan
Faculty of Engineering & Technology
Mechanical Engineering Department
Amman 11942, Jordan

Heat Losses Minimization from Hydrogen Fueled 4-Stroke Spark Ignition Engines

This paper presents an analytical study to minimize the heat lost during the power stroke of hydrogen-fueled, 4-stroke spark ignition engine. The effects of various design and operating parameters like engine speed, equivalence ratio, ignition timing, compression ratio and spark plug location on heat losses was studied. Then, the effect of heat loss on the engine's performance and emission characteristics was conducted with aim to minimize it. The study showed that the percentage heat loss decreased with increase in engine speed. Further, changing the compression ratio from 7 to 11 produced change of around 2-3% in percentage heat loss, while changing the spark plug location from periphery to center produced change of around 1-1.5% in percentage heat loss with maximum change occurring at lean mixtures. Changing the ignition timing from 50 to 10 degrees bTDC changed the percentage heat loss by more than 4%. As for the effect of percentage heat loss on the engine performance and emission characteristics, it was found that some of the heat must be allowed to be transferred from the cylinder to enhance the engine performance. This amount of heat loss varies with engine speed and equivalence ratio. It was found to be higher at higher engine speeds. Beyond this specific value, the engine performance and emission characteristics deteriorate.
Keywords: *hydrogen engine simulation, alternative fuels, percentage heat loss, engine simulation*

Introduction

Never before did Jordanians experience such a soaring temperature that exceeded $40^{\circ}C$ as they did during the summer of the year 2000. This was accompanied with acute shortage of rain and greater disturbance in the ecological system of Jordan. Several studies gave different reasons to this new phenomenon. Many agree that after the unprecedented increase in the number of automobiles in the streets, drastic changes to the ecological system and even an increase in the respiratory-related diseases started to be strongly felt in Jordan.

This was accompanied with the greater political disturbances in the region which made the fuel supply to Jordan politically oriented. These besides other reasons encouraged researchers to look for other sources of energy that are safe and environmentally friendly such as solar, wind, alternative fuels and other new and clean sources of energy.

According to the best estimates, the world's fossil fuel (coal, petroleum and natural gas) production, which meets about 80% of our energy requirements today, will start to decline in 20-30 years time. The petroleum and natural gas production is already decreasing in parts of the world like United States. On the other hand, since the demand for energy is ever increasing as the nations of the world try to better their living standards; alternative energy sources are being considered. Research regarding their conversion into usable forms of energy is being accelerated.

Since fossil fuels cause great damage to the environment through the greenhouse effect, ozone layer depletion, acid rains, air pollution, oil spills. etc., the research emphasis is on the clean energy sources and carriers.

A quick look at the currently available alternatives, they are found to be classified into two main categories:
1. Long term alternatives, and,
2. Short term alternatives.

Liquefied petroleum gas, natural gas, alcohol and many other hydrocarbon fuels are considered among the short term solutions since they are finite in nature and are derived from sources that are finite and suffering from overstress and exhaustion.

Hydrogen, on the other hand, represents the long-term solution due to its unique properties. It is produced from variety of energy sources such as water and using variety of energy sources such as solar, nuclear and fossil. It also can be converted to useful forms of energy efficiently and with least detrimental environmental effect.

In spite of the numerous advantages of hydrogen, still more research has to be performed to try to clearly understand the combustion characteristics of this new fuel to enable researchers exploiting its properties to their best and therefore, optimize the engine design for hydrogen.

Nomenclature

A = *piston cross-section area, m^2*
a = *constant used in Annand's equation*
b = *constant used in Annand's equation*
C_v = *specific heat at constant volume, $J/(kg\ K)$*
C_p = *specific heat at constant pressuree, $J/(kg\ K)$*
D = *cylinder diameter, m*
e = *specific internal energy, $J/(kg)$*
Ea = *activation energy*
K_q = *thermal conductivity , $W/(m\ K)$*
N = *Engine speed, rev per minute*
P = *pressure,bar*
Q = *heat transfer rate, W*
R = *universal gas constant, $J/(kg.K0$*
$Rmol$ = *gas constant , $J/(kmol.K)$*
Re = *Reynolds number , dimensionless*
S = *stroke length, m*
T = *absolute temperature, K*
U_t = *turbulent flame speed , m/s*
V = *cylinder volume, m^3*
W = *work, J*
X_f = *mole fraction of fresh mixture*

Greek Symbols

θ = *crank angle, deg.*
μ = *dynamic viscosity, $kg/(m\ s)$*
ϕ = *equivalence ratio, dimensionless*

Subscripts

b   burnt
u   unburnt

Hydrogen Properties

Some of the key overall properties of hydrogen that are relevant to its employment as an engine fuel are listed in Table 1.

It is evident that hydrogen is a remarkably light gaseous fuel that requires on volume basis the least amount of air for stoichiometric combustion (2.39 versus 59.6 for iso-octane); while on mass basis it requires the highest relative mass of air. Its combustion is also associated with a substantial molar contraction of around 15%. Its heating value on mass basis is the highest; but on volume basis it is the lowest. Also, since its product of combustion in air is mainly water, there is significant difference between its higher and lower heating values. However, its energy release by combustion per unit mass of stoichiometric mixture is one of the highest.

Hydrogen has some remarkably high values of the key properties for transport processes, such as kinematic viscosity, thermal conductivity and diffusion coefficient. Such properties together with its extremely low density and low luminosity help to give hydrogen its unique diffusive and heat transfer characteristics.

Table 2 lists some combustion properties that have much influence on the potential behavior of hydrogen as a fuel in general and for engine applications in particular. It can be seen that hydrogen has a remarkably wide flammable mixture range in air to permit extremely lean or rich mixtures support combustion. It requires also a remarkably low minimum amount of energy to effect ignition with extremely fast resulting flames with air. However, the values of its spontaneous ignition temperatures are quite similar to those for gasoline and the value for the maximum adiabatic combustion temperature in air is slightly little higher.

Based on the above discussion it can be said that the engine design has to be modified to suit the properties of the new fuel. Not doing so (i.e. re-designing the engine based on its properties) may cause the following:

- High rate of pressure rise due to rapid combustion process and hence rapid rate of pressure rise, which may lead to knocking.
- Early completion of combustion process before top dead center (hereinafter referred to as TDC) or while the piston is rising towards TDC. This leads to loss of power and excess heat loss.

Table (1). Properties of hydrogen (Karim, 2003).

Property	Hydrogen
Density at 1 atm and 300 K (kg/m^3)	0.082
Stoichiometric composition in air (% Volume)	29.53
Kinematic Viscosity at 300 K (mm^2/s)	110
Research Octane Number	130
Lower Heating Value (MJ/kg)	119.7
Thermal conductivity at 300 K (mW/m K)	182.0
Diffusion coefficient into air at NTP (cm^2/s)	0.61
Stoichiometric fuel/air mass ratio	0.029

Table (2). Some comparative combustion of hydrogen (Karim, 2003).

Property	Hydrogen
Flammability Limits (% Volume)	4-75
Minimum Ignition Energy (mJ)	0.02
Laminar Flame Speed at NTP (m/s)	1.9
Adiabatic Flame Temperature (K)	2318
Auto-ignition Temperature (K)	858
Quenching Gap at NTP (mm)	0.64

Brief Description of Simulation Model

The main program consists of two main stages: (1) The pipe calculations, and (2) the cylinder calculations. The cylinder calculations are further subdivided into two main stages: (1) power cycle and (2) gas exchange process. The power cycle is subdivided into three main stages: (1) compression, (2) ignition or combustion and (3) expansion or power stroke. Finally, the expansion stroke is further subdivided into (1) expansion with two zones (burned and unburned), and (2) expansion of full products. The model was modified with the inclusion of the gas exchange model, the turbulent combustion model, and the inclusion of the calculation of the friction parameters of various parts of the engine. Since describing the complete model would make this paper extremely lengthy and would bring it out of scope of the main topic, below is a brief description of the model.

Compression

The pressure and temperature in this stroke is calculated using the first law of thermodynamics equations and the equation of state as given in (Gupta, 1995):

$$\frac{dp}{d\theta} = \left\{ \frac{R}{C_V}\left(\frac{dQ}{d\theta}\right) - p\frac{dV}{d\theta}\left(\frac{R}{C_V}+1\right) \right\}/V \tag{1}$$

$$\frac{dT_u}{d\theta} = T_u\left(\frac{1}{V}\cdot\frac{dV}{d\theta} + \frac{1}{p}\cdot\frac{dp}{d\theta}\right) \tag{2}$$

$$\frac{dW}{d\theta} = p\frac{dV}{d\theta} \tag{3}$$

The heat transfer rate from the gas to wall is calculated using Annand's equation (Annand, 1963):

$$\frac{Q}{A} = \frac{a\,k_q}{D}(R_e)^b(T_u - T_w) \tag{4}$$

where $K_q = C_P\mu/0.7$. The variables are continuously updated during calculation using the general formula:

$$X_{n+1} = X_n + (dX/d\theta)\Delta\theta \tag{5}$$

where "x" is any variable. The numerical procedure used for this purpose is the Runge-Kutta Method.

Ignition

The calculations then proceed in three phases. Firstly, the initiation of the combustion, then the subdivision of the combustion chamber into two zones separated by spherical flame front and, finally a single zone encompassing the whole of the combustion chamber. To initiate the combustion a unit mass of the cylinder content is considered to burn at constant volume. The internal energy of the initial reactants is set equal to the internal energy of the products. The first guessed value of the burnt temperature "T_b" is calculated using the Annand's equation (Gupta, 1995) as below:

$$T_b = T_u + 2500 * \phi * X_f \qquad \text{for } \Phi \leq 1.0 \tag{6}$$

$$T_b = T_u + 2500 * \phi * X_f - 700 * (\phi-1.0)*X_f \qquad \text{for } \Phi > 1.0 \tag{7}$$

$$T_b = T_b - \delta\,T_b \tag{8}$$

where, $\delta T_b = (e_b - e_u) / C_{vb}$. Further, the following turbulent flame speed equation for pure hydrogen given by (Al-Janabi, 1999) was used:

$$Ut = 5000 * \left[\frac{0.1*N*D*S*P}{T_b^{1.67}}\right]^{0.4} * (T_b^{0.41} * T_u^{1.25}) * (Rmol / Ea) *$$

$$\left[\frac{X_f\left(1 - \phi * \left(1 - \frac{Rmol * T_b^2}{Ea * (T_b - T_u)}\right)\right)}{\phi}\right]^{0.5} * \exp\left(\frac{-Ea}{2.0 * Rmol * T_b}\right) \quad (9)$$

Species Formation

The governing equations for the mechanism of NO formation are given in (Raine, 1995):

$$\begin{aligned}
&(1)\ N+NO \Longleftrightarrow N_2+O \quad Kf1 = 3.1*10^{10} * E^{(-160/T)}\ m^3/kmols \\
&(2)\ N+O_2 \Longleftrightarrow NO+O \quad Kf2 = 6.4*10^6 * T * E^{(-3125/T)}\ m^3/kmols \\
&(3)\ N+OH \Longleftrightarrow NO+H \quad Kf3 = 4.2*10^{10}\ m^3/kmols \\
&(4)\ H+N_2O \Longleftrightarrow N_2+OH \quad Kf4 = 3.0*10^{10} * E^{(-5350/T)}\ m^3/kmols \\
&(5)\ O+N_2O \Longleftrightarrow N_2+O_2 \quad Kf5 = 3.2*10^{12} * E^{(-18900/T)}\ m^3/kmols \\
&(6)\ O + N_2O \Longleftrightarrow NO+NO \quad Kf6 = Kf5\ m^3/kmols \\
&(7)\ N_2O+M \Longleftrightarrow N_2+O+M \quad Kf7 = 10^{12} * E^{(-30500/T)}\ m^3/kmols
\end{aligned} \quad (10)$$
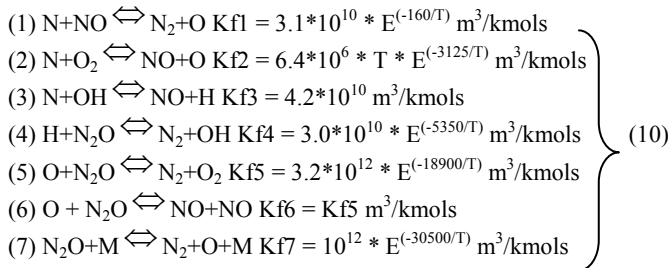
In these equations the rate constants (Kfi) are all in $m^3/kmols$. 'M' is a third body which may be involved in the reactions, but is assumed to be unchanged by the reactions. 'M' can be assumed to be N_2. These equations can be applied to the zone containing "burned" products, which exists after the passage of the flame through the unburned mixture. It will be assumed that H and OH, and O and O_2 are in equilibrium with each other; these values can be calculated by the methods given in (Winterbone, 1997). Referring to equations (10) the net rate for NO can be derived as follows:

$$Kf1[N][NO]+Kb1[N2][O] = -\alpha\beta Kf1[N]_e[NO]_e+Kb1[N2]_e[O]_e \quad (11)$$

But,
$Kf1[N]_e[NO]_e = Kb1[N2]_e[O]_e = R1$

So the net rate from the first equation of the set of equations (10) becomes $-\alpha\beta R1 + R1$. Using similar procedure for the rest of equations of (10) involving NO, N_2O and finding R2 through R7 and using the following expressions

$$\beta = \frac{R_1 + \alpha(R_2 + R_3)}{(\alpha R_1 + R_2 + R_3)} \quad \text{and} \quad \gamma = \frac{R_4 + R_5 + \alpha^2 R_6 + R_7}{(R_4 + R_5 + R_6 + R_7)}$$

gives the following expression for the rate of formation of (NO) as :

$$\frac{1}{V} \cdot \frac{d}{dt}[NO].V = 2.(1-\alpha^2)\left[\frac{R_1}{1+\alpha\frac{R_1}{R_2+R_3}} + \frac{R_6}{1+\frac{R_6}{R_4+R_5+R_7}}\right]$$

Model Modification and Verification

Though this model was verified for the gasoline-fueled engines (Yamin, 1998 & 2000), there is a need to verify the model for the case of Hydrogen-fueled engines. This was the first part of this study. For this part the thermodynamic, physical, chemical and coefficients of certain thermophysical properties of hydrogen were incorporated since the properties of fuels affect the performance of the engine. Some of the Hydrogen properties are included in Appendix (A)

Then, the experimental data of the Ricardo E6/T variable compression ratio engine with CR = 7.5, $\phi = 1.0$ and MBT spark timing were compared with the calculated data. The results are shown in Fig. 1 e 2. These figures clearly show that the model can predict the performance of the engine to a good degree of accuracy.
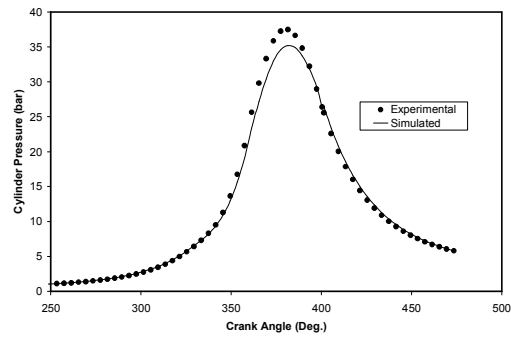
Figure 1. Comparison between the experimental and calculated modeled cylinder pressure variations at CR = 7.5, MBT spark timing, WOT and stoichiometric mixture.
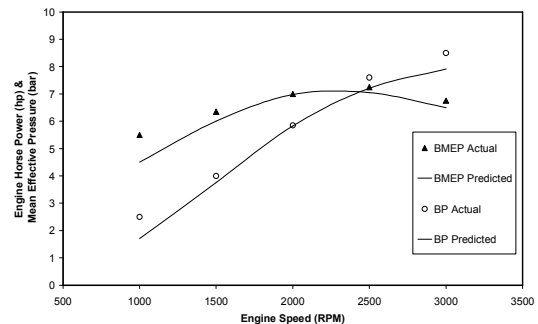
Figure 2. Comparison between the experimental and modeled brake horse power and mean effective pressure variations CR = 7.5, MBT spark timing, WOT and stoichiometric mixture.

Results and Discussion

One of these parameters investigated is the effect of percentage heat losses on engine performance and emission characteristics. This was done analytically using SimHydrogEn (Simulation of Hydrogen Engine) code developed by the author (Yamin, 2006). The investigation was carried out in two phases. The first phase discussed the effect of certain engine design parameters on the percentage heat loss. These parameters investigated were compression ratio (CR) varied from 7:1 to 11:1, engine speed was varied from 1000 RPM to 3000 RPM, equivalence ratios (ϕ) varied from $\phi = 0.7$ to $\phi = 1.2$, spark plug location (XSP) which is defined as the ratio of the distance between the spark and the nearest wall to the cylinder diameter, varied from original design of XSP = 0.08 to center, the ignition timing was varied from 10 to 50 degrees before top dead center (BTDC). The study was conducted under wide open

throttle (WOT). Some of the Ricardo E6/T Variable Compression Ratio engine specifications are: single cylinder, 4-stroke, water-cooled, variable compression ratio and spark ignition engine. It has cylinder bore of 76.20 mm, stroke length of 110.0 mm, connecting rod length of 241.3 mm, mean Inlet valve diameter of 35.0 mm and mean exit valve diameter of 30.0 mm.

The second phase was conducted after finding the MBT angle for every engine speed, taking CR = 9:1 and under WOT. The results of the first part of the study are presented below.

Effect of Spark Plug Location

Figure (3) shows the effect of spark plug location on the percentage heat losses at different equivalence ratios. As it may be seen from the graph, the percentage heat losses decreases as the spark plug is moved from the edge (XSP=0.08) to the center (XSP=0.5). This is mainly due to the reduction in the combustion duration; hence, less time would be available for the products of combustion to lose its heat to the surroundings. This effect is more dominant at leaner equivalence ratios because of the longer combustion duration. Further, it may be noticed that the percentage heat losses reduces (at XSP = 0.5) as the mixture is made slightly richer than 0.7. This is because of the poor combustion of the fresh charge at ϕ = 0.7. These losses further drop as the mixture is enriched beyond stoichiometric due to poorer combustion and lower energy release.
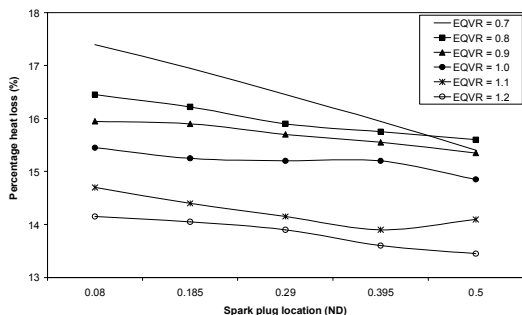
Figure 3. Effect of spark plug location on the percentage heat loss at different equivalence ratios with CR = 9.0, 2500 rpm, MBT spark timing and WOT.

Effect of Compression Ratio

Figure (4) shows the effect of compression ratio on percentage heat losses at different equivalence ratios for a peripheral spark location. As shown, percentage heat loss increases as the compression ratio increases; this is mainly due to higher temperature and pressure at the end of compression nearer to TDC.
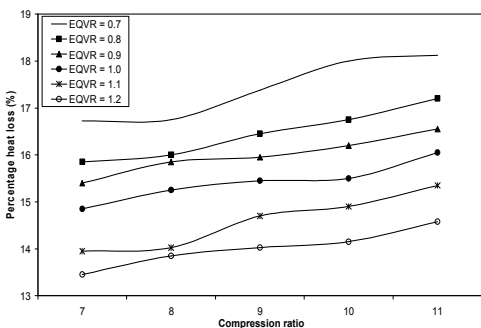
Figure 4. Effect of compression ratio on percentage heat losses at different equivalence ratios with CR = 9.0, 2500 rpm, MBT spark timing and WOT.

Effect of Engine Speed

Figure (5) shows the effect of engine speed on the percentage heat loss at different equivalence ratios for a peripheral spark location. The figure clearly shows the effect of increased turbulence at higher engine speeds which results in better combustion and lesser combustion duration, hence, lower percentage of heat loss.
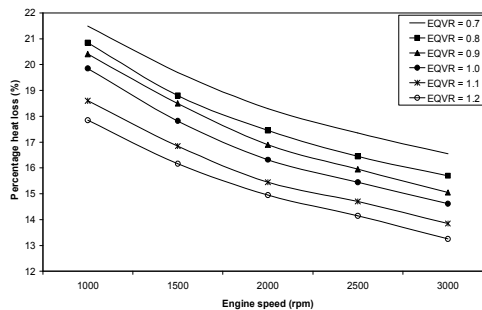
Figure 5. Effect of engine speed on the percentage heat loss at different equivalence ratios with CR = 9.0, 2500 rpm, MBT spark timing and WOT.

Effect of Spark Timing

Figure (6) shows the effect of spark timing on percentage heat loss at different equivalence ratios for a peripheral spark location. It clearly shows that more the spark advance the more is the percentage heat loss. This is because of the earlier completion of combustion within TDC hence more time is available for the product of combustion to impart its heat to the surroundings, as shown in Fig. 7 e 8.

Now, after discussing the effect of various design parameters on heat losses, let us now discuss the effect of heat losses on the performance and emission characteristics of the engine.
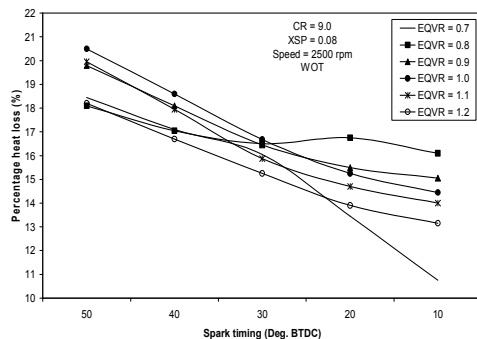
Figure 6. Effect of spark timing on the percentage heat loss at different equivalence ratios with CR = 9.0, 2500 rpm, MBT spark timing and WOT.
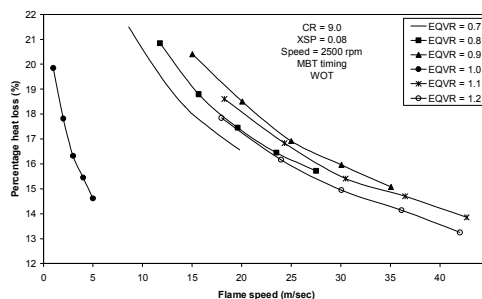
Figure 7. Effect of flame speed on the percentage heat loss at different equivalence ratios with CR = 9.0, 2500 rpm, MBT spark timing and WOT.
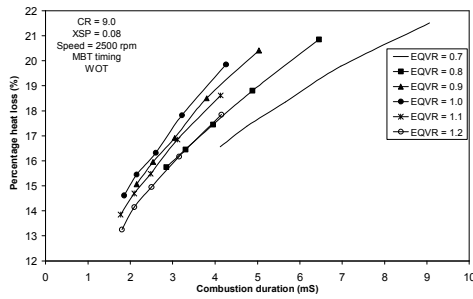
Figure 8. Effect of combustion duration on the percentage heat loss at different equivalence ratios with CR = 9.0, 2500 rpm, MBT spark timing and WOT.

Effect of Percentage Heat Losses on Peak Cycle Pressure and Temperature

Figure (9) shows the effect of percentage heat loss on the maximum cylinder pressure and unburnt temperature. They clearly show that as the percentage heat loss increases, the peak pressure and temperature increases first then decreases. This is thought to be due to the effect of dissociation that is suppressed as some of the heat generated by the combustion of the fuel gets dissipated. Later, as the amount of heat lost increases, the peak cycle temperature and pressure decreases. This clearly shows that slight heat loss helps in improving the combustion process as it suppresses the dissociation losses.
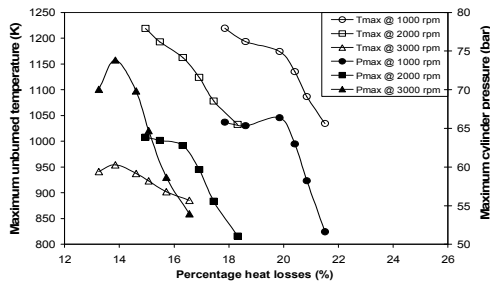
Figure 9. Percentage heat loss effect on the maximum cylinder temperature and pressure at different engine speeds with CR = 9.0, 2500 rpm, MBT spark timing and WOT.

Effect of Percentage Heat Losses on Engine Power

Figure (10) shows the effect of percentage heat loss on brake mean effective pressure (BMEP) and brake horse power (BHP). The trend followed by the BMEP and BHP is similar to that followed by peak cycle pressure.
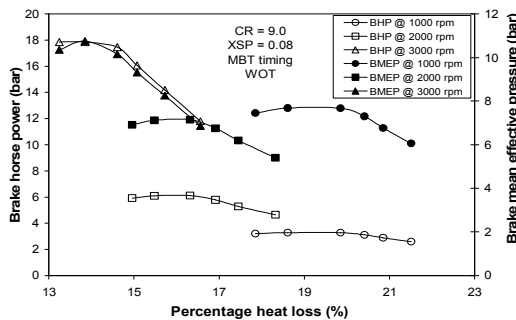
Figure 10. Effect of percentage heat loss on the BHP & BMEP at different engine speeds with CR = 9.0, 2500 rpm, MBT spark timing and WOT.

Effect of Percentage Heat Losses on Engine's Economy

Figures 11 e 12 show the effect of percentage heat loss on both brake specific fuel consumption (BSFC) and brake thermal efficiency. As seen from the figures, both of these factors improve at first with little heat lost but then deteriorates as further heat is lost to the surroundings.
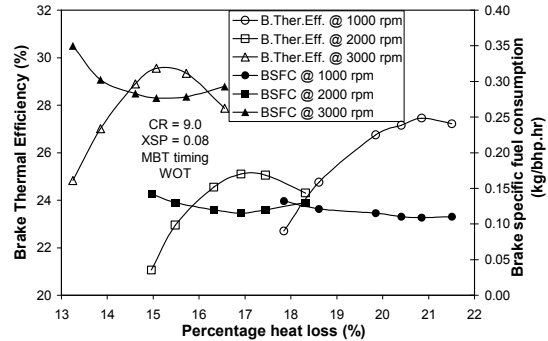
Figure 11. Effect of percentage heat loss on BSFC & brake thermal efficiency at different engine speeds with CR = 9.0, 2500 rpm, MBT spark timing and WOT.
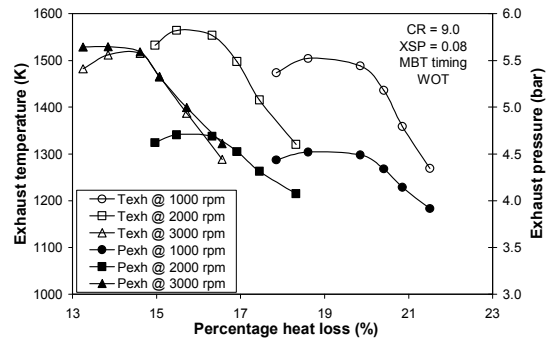
Figure 12. Effect of percentage heat loss on exhaust pressure and temperature at different engine speeds with CR = 9.0, 2500 rpm, MBT spark timing and WOT.

Effect of Percentage Heat Losses on Nitrogen Oxide Emission Level

Figure (13) show the effect of the percentage heat loss on the NO level. It clearly shows that as the percentage heat lost increases, NO level increases up to certain limit where it starts to decrease. This is mainly related to the improved combustion at lesser percentages of heat loss.
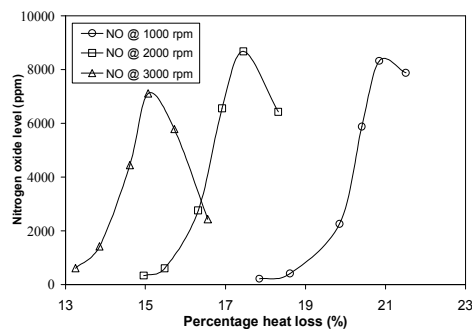
Figure 13. Effect of percentage heat loss on NO level at different engine speeds with CR = 9.0, 2500 rpm, MBT spark timing and WOT.

Discussion of the Results

These results show that not all the heat liberated from the combustion of the fuel should be allowed to remain inside the engine which is a principle followed by the researchers in the area of LHR engines. Though theoretically, if all the heat is allowed to remain and participate in the power development process, it would improve the engine's performance, however, the practical results obtained from the LHR engines disagreed with this theoretical assumption. Therefore, it is seen from the results of this study that some parts of the heat must be allowed to escape in order to suppress certain losses such as variable specific heat and dissociation losses. This would improve the engine's performance. However, the study further shows that excessive heat loss is not favorable.

From the engine design parameters' point of view, the use of central spark location, lower compression ratios, retarded spark advance and higher engine speeds lead to lower percentage heat losses. This, however, is not free from troubles as these parameters highly affect the engine performance. Therefore, greater care must be taken when selecting these parameters.

Conclusion

1. Not all the heat liberated from the combustion of the fresh charge is useful to the engine. Part of it must be dissipated if the engine's performance has to improve.
2. Further study has to be conducted to see for the effect of other design parameters such as valve geometry, diameter, lift and numbers and correlate them with the above study to reach to a better understanding about its total effect on the engine's performance.
3. The percentage heat loss decreased with increase in engine speed. Further,
4. Changing the compression ratio from 7 to 11 produced change of around 2-3% in percentage heat loss, while changing the spark plug location from periphery to center produced change of around 1-1.5% in heat loss with maximum change occurring at lean mixtures.
5. Changing the ignition timing from 50 to 10 degrees BTDC changed the heat loss by more than 4%.
6. It was found that some of the heat must be allowed to be transferred from the cylinder to enhance the engine performance. This amount of heat loss varies with engine speed and equivalence ratio. It was found to be higher at higher engine speeds. Beyond this specific value, the engine performance and emission characteristics deteriorate.
7. A final point to notify is that the data for the NO emission verification was not given in this paper. Hence, there is need to verify the model for the emission levels.

References

Karim, G.A., 2003, "Hydrogen as spark ignition engine fuel', International Journal of Hydrogen Energy, Vol.28, pp.569-577

Gupta, H. N. et.al, 1995, "Computer Simulation of Power Cycle for Spark-Ignition Engine", IE (I)-Journal-MC, Vol. 76, November.

Annand, W. J. D., 1963, "Heat Transfer in the Cylinders of Reciprocating Internal Combustion Engines", Proc. Instn. Mech. Engrs. Vol. 177, No. 36.

Al-Janabi H.A.K.S, and Al-Baghdadi, M.A., 1999, "A prediction study of the effect of hydrogen blending on the performance and pollutants emission of a four stroke spark ignition engine". International Journal of Hydrogen Energy, 24 , pp. 363-375.

Raine, R.R., Stone, C.R. and Gould, J., 1995, "Modeling of Nitric Oxide Formation in Spark Ignition Engines with a Multi-zone Burned Gas", Journal of Combustion and Flame, Vol. 102, No.3, pp. 241-255.

Winterbone, D. E., 1997, Advanced Thermodynamics for Engineers. John Wiley & Sons.

Yamin, J.A.A. Gupta, H.N., Bansal, B.B. and Srivastava, O.N., 1998, "Analytical Studies to Optimize the Design and Operating Parameters for Hydrogen-Fuelled 4-Stroke Spark Ignition Engines", Paper presented in the Hydrogen Energy Conference, Argentina.

Yamin, J.A.A., Gupta, H.N., Bansal, B.B. and Srivastava, O.N., 2000, "Effect of combustion duration on the performance and emission characteristics of a spark ignition engine using hydrogen as a fuel", International Journal of Hydrogen Energy, Vol.25, pp. 581-589.

Jehad A.A. Yamin, 2006, "Comparative Study Using Hydrogen and Gasoline as fuels for 4-Stroke Spark Ignition Engines: Combustion Duration Effect", International Journal for Engineering Research, Vol.30, No.14, pp.1175 - 1187

Appendix (A)

Hydrogen Fuel Data :

Internal Energy Coefficients for polynomial expression (Winterbone, 1997) where

$$E(T) = R_{mol} \left[\sum_{i=1}^{i=5} M_i \left[\left[\sum_{j=1}^{j=5} a_{ij} T^j \right] - T \right] + \frac{h_{oi}}{R_{mol}} \right] :$$

	3000 > T > 500 K	3000 > T > 6000 K
a1	3.43328	3.21299
a2	-8.18100E-06	2.87156E-04
a3	9.66990E-08	-2.28839E-08
a4	-1.44392E-11	7.66560E-13
a5	0.0	0.0
h_o	0.0	0.0

Viscosity Coefficient (Kg/m.s):	8.6E-06
Calorific Value (kJ/Kg):	119617
Annand's Constants:	
a	0.40
b	0.70
c	0.4284E-011 (kW/m^{2}K^4)